Science of the Total Environment 917 (2024) 170331

Contents lists available at ScienceDirect

Science of the Total Environment

journal homepage: www.elsevier.com/locate/scitotenv

# Toxicity and underlying lipidomic alterations generated by a mixture of water disinfection byproducts in human lung cells

Mahboubeh Hosseinzadeh [a,*], Cristina Postigo [b,c], Cinta Porte [a]

[a] Environmental Chemistry Department, Institute of Environmental Research and Water Assessment, IDAEA -CSIC-, C/ Jordi Girona, 18-26, 08034 Barcelona, Spain
[b] Technologies for Water Management and Treatment Research Group, Department of Civil Engineering, University of Granada, Avda. Severo Ochoa s/n, Granada 18071, Spain
[c] Institute for Water Research (IdA), University of Granada, Ramón y Cajal 4, 18071 Granada, Spain

## HIGHLIGHTS

- Exposure to DBP mixture did not affect the viability of A549 cells.
- Increased ROS generation and micronuclei formation detected in exposed cells.
- Increased accumulation of TGs detected in lung cells after exposure to the mixture.
- DBP mixture exposure altered the lipidomic composition of extracellular vesicles.

## GRAPHICAL ABSTRACT

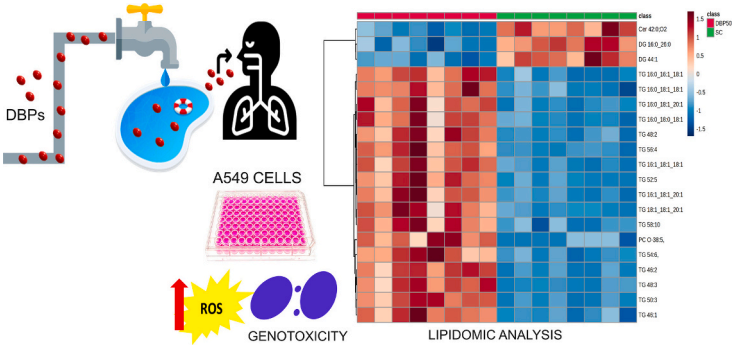


## ARTICLE INFO

Editor: Jay Gan

*Keywords:*
A549 cell line
Mixture toxicity
Haloacids
Halophenols
Micronuclei
Lipidome

## ABSTRACT

Complex mixtures of disinfection by-products (DBPs) are present in disinfected waters, but their mixture toxicity has been rarely described. Apart from ingestion, DBP exposure can occur through inhalation, which may lead to respiratory effects in highly exposed individuals. However, the underlying biological mechanisms have yet to be elucidated. This study aimed to investigate the toxicity of a mixture of 10 DBPs, including haloacetic acids and haloaromatics, on human alveolar A549 cells by assessing their cytotoxicity, genotoxicity, and impact on the cell lipidome. A DBP mixture up to 50 μM slightly reduced cell viability, induced the generation of reactive oxygen species (ROS) up to 3.5-fold, and increased the frequency of micronuclei formation. Exposure to 50 μM DBP mixture led to a significant accumulation of triacylglycerides and a decrease of diacylglycerides and phosphatidylcholines in A549 cells. Lipidomic profiling of extracellular vesicles (EVs) released in the culture medium revealed a marked increase in cholesterol esters, sphingomyelins, and other membrane lipids. Overall, these alterations in the lipidome of cells and EVs may indicate a disruption of lipid homeostasis, and thus, potentially contribute to the respiratory effects associated with DBP exposure.

* Corresponding author.
*E-mail address:* mhotam@cid.csic.es (M. Hosseinzadeh).

https://doi.org/10.1016/j.scitotenv.2024.170331
Received 18 October 2023; Received in revised form 15 January 2024; Accepted 19 January 2024
Available online 24 January 2024

## 1. Introduction

Water disinfection aims to kill or inactivate pathogens that cause water-borne diseases (Richardson and Plewa, 2020). However, the use of chemicals for this purpose (e.g., chlorine, chloramines, chlorine dioxide, ozone) unintentionally results in the formation of disinfection by-products (DBPs) after their reaction with the organic and inorganic matter present in the water (Richardson, 2011). Trihalomethanes (THMs) and haloacetic acids (HAAs) are the DBP classes mostly formed in chlorinated water (Hu et al., 2021), and thus, the most investigated ones. Research on THMs and HAAs has led to the inclusion of four THMS (THM4) and five HAAs (HAA5) among the very few DBPs regulated in drinking water in the USA (USEPA, 2010) and the European Union (European Commission, 2020), and practically, worldwide. Nevertheless, the enhanced sensitivity and specificity of advanced analytical techniques and detection methods have allowed researchers to uncover the formation of hundreds (over 700) of chemical compounds in disinfected water (Li and Mitch, 2018). Some of these newly discovered DBPs have been reported to be more toxic than regulated DBPs (Jeong et al., 2012; Li and Mitch, 2018; Richardson and Plewa, 2020). Non-regulated emerging DBPs include halogenated and non-halogenated nitrogen-containing compounds, iodinated compounds, and haloaromatic compounds, among others (Richardson et al., 2010; Kosaka et al., 2017; Yang et al., 2019). The haloaromatic fraction constitutes about 30 % of the total organic halogenated material (TOX) present in chlorinated water (Han et al., 2021).

Nowadays, only about 15 % of the known DBPs have been toxicologically characterized, and none of them can individually explain the increased risk of bladder cancer (Cantor et al., 2010) and adverse developmental effects (Tardiff et al., 2006) reported in epidemiological studies (Hrudey, 2009; Villanueva et al., 2015). Thus, it is likely that these effects may result from the mixture of known and yet unknown DBPs present in water, with ~70 % of the halogenated compounds in chlorine-disinfected water still unidentified (Li and Mitch, 2018). Intriguingly, several studies have shown that exposure to multiple DBPs may result in synergistic effects on cytotoxicity, oxidative response, and genotoxicity (Pereira et al., 1997; Lu et al., 2018; Chen et al., 2019; Liu et al., 2022). Conversely, antagonistic effects have also been reported in certain cases (Lu et al., 2018).

In addition to drinking water, exposure to DBPs through dermal absorption or inhalation raises concerns (Nuckols et al., 2005; Font-Ribera et al., 2010; Cardador and Gallego, 2011; Chowdhury, 2013). The inhalation pathway is relevant not only for volatile DBPs, but also for less volatile DBPs (e.g. haloacetic acids) that can be highly concentrated in the air of intensively disinfected indoor areas (Lou et al., 2021) or indoor swimming pools (Yang et al., 2018). Exposure to DBPs at indoor pools has been associated with a higher prevalence of respiratory effects, such as asthma or other airway symptoms, among swimmers and pool workers (Thickett et al., 2002; Goodman and Hays, 2008; Villanueva and Font-Ribera, 2012; Chu et al., 2013; Fornander et al., 2013). While no significant changes in immune or genotoxic markers (Pedersen et al., 2009; Font-Ribera et al., 2010, 2019) and lung damage markers (Llana-Belloch et al., 2016) have been observed after swimming in chlorinated pools, acute changes in cytokine and chemokine secretion patterns have been reported (Vlaanderen et al., 2017). The possible underlying cause of the observed respiratory effects may be the disruption of surfactant homeostasis in lung cells due to DBP exposure, an area that requires further investigation. Notably, type 2 cells in the alveoli play a crucial role in the biosynthesis and recycling of surfactant lipids, which are essential for respiration (Zemski Berry et al., 2017; Agudelo et al., 2020). This hypothesis gains support from previous studies where several pollutants have been shown to disrupt surfactant homeostasis in lung cells (Sánchez-Soberón et al., 2018; Rossner et al., 2020). Among these lipids, phospholipids play an important role in lung inflammation and are essential to reduce surface tension in alveoli, thereby facilitating gas exchange (Zemski Berry et al., 2017).

This study delves into the understudied area of complex mixtures of DBPs and their toxicity through inhalation. It addresses this knowledge gap by assessing the toxicity of a mixture of ten DBPs, encompassing both haloaliphatic and haloaromatic DBPs, on human alveolar type 2 lung cells. Among the haloaliphatic DBPs, the widely investigated monohaloacetic acids (HAAs), viz., iodoacetic (IAA), bromoacetic (BAA), and chloroacetic acid (CAA), were prioritized. The most abundant HAA in chlorinated DBP mixtures, dichloroacetic acid (DCAA), and HAAs that are expected to be toxic due to the presence of iodine in their structure (chloroiodoacetic acid (CIAA) and diiodoacetic acid (DIAA)) were also selected. As previously noted, HAAs is a major DBP class in chlorinated water, included in most drinking water regulations worldwide. The selected haloaromatic DBPs included four emerging DBPs belonging to three different chemical classes: 2,6-dichloro-1,4-benzoquinone (DCBQ), 2,4,6-trichlorophenol (TCP), 2,4,6-tribromophenol (TBP), and 3,5-dibromo-4-hydroxybenzaldehyde (DBHB). DCBQ, TCP, and TBP have shown elevated toxicity compared to other DBPs, including regulated ones (Li et al., 2015; Miao et al., 2022; Pérez-Albaladejo et al., 2024). Since concentrations of individual aliphatic and aromatic DBPs vary several orders of magnitude in disinfected waters, depending on the source of water, disinfectant used, and disinfection conditions, exposure tests were conducted at equimolar concentrations of the individual DBPs (1–5 μM), with a maximum total DBP concentration of 50 μM. It is worth noting that DCAA levels in swimming pool waters can reach up to 2400 μg/L (18.61 μM) (Yeh et al., 2014), whereas maximum concentrations in drinking water are commonly 100 times lower (Kargaki et al., 2020). In this context, this study aimed at uncovering the mechanisms behind the toxic effects associated with DBP inhalation by assessing cytotoxicity, the generation of reactive oxygen species (ROS), genotoxicity, and changes in the lipidome of human alveolar type 2 lung cells.

## 2. Materials and methods

### 2.1. Chemicals and solutions

Dulbecco's Modified Eagle Medium-high glucose (DMEM) was from Sigma-Aldrich (Merck, Darmstadt, Germany), fetal bovine serum (FBS), penicillin, streptomycin, 0.25 % trypsin-ethylenediaminetetraacetic acid (EDTA), and Dulbecco's phosphate-buffered saline with Ca and Mg (DPBS) were from Gibco-BRL Life Technologies, (Paisley, Scotland, UK). 2′,7′-Dichlorodihydrofluorescein diacetate (H2DCF-DA), 3-morpholinosydnonimine hydrochloride (SIN-1), Alamar Blue (AB), and 5-carboxyfluorescein diacetate acetoxymethyl ester (CFDA-AM) were from Invitrogen (Paisley, UK). Dimethyl sulfoxide (DMSO) and bisbenzimide 33342 Hoechst were purchased from Sigma-Aldrich. Salts to prepare phosphate-buffered saline (PBS), viz., NaCl, KCl, $Na_2HPO_4$, and $KH_2PO_4$, were obtained from Merck, Darmstadt, Germany.

The internal standards for lipidomic analyses, namely 16:0-d31–18:1 phosphatidylcholine (PC), 17:0 lysophosphatidylcholine (LPC), C18 (Plasmalogen)-18:1 (d9) phosphatidylcholine (PC-P), 16:0-d31–18:1 phosphatidylethanolamine (PE), 16:0-d31–18:1 phosphatidylserine (PS), 16:0-d31–18:1 phosphatidylinositol (PI), d31–18:1 phosphatidylglycerol (PG), 16:0d31 sphingomyelin (SM), 16:0d31 ceramide (Cer), 1,3–17:0-d5 diacylglycerol (DG), 1,2,3–17:0 triacylglycerol (TG), and 16:0 cholesteryl-d7-ester (CE) were acquired from Avanti Polar Lipids, Inc. (Alabama, US).

As for the selected DBPs, IAA, BAA, CAA, DCAA, DCBQ, TCP, TBP, and DBHB were purchased from Sigma-Aldrich, whereas CIAA and DIAA were obtained from CanSyn Chem. Corp (Toronto, Canada). The stock solution mixture of 10 DBPs was prepared in DMSO at a concentration of 10 mM. This solution contained the individual DBPs at a concentration of 1 mM. Detailed information on selected DBPs is presented in Table S1.

### 2.2. Cell culture

The human alveolar epithelium adenocarcinoma cell line A549

(CCL-185™, ATCC, LGC Standards SLU, Barcelona, Spain) was cultured in DMEM supplemented with 10 % inactivated FBS, and penicillin-streptomycin (10 U/mL-10 μg/mL). Cells were maintained in a humidified incubator at 37 °C and 5 % $CO_2$ atmosphere. For experiments, cells were trypsinized (0.25 % *w/v*) and seeded when they reached 90 % confluence.

### 2.3. Cell viability

AB and CFDA-AM were used to evaluate the effect of the DBP mixture on cell viability (Schirmer et al., 1997). A549 cells ($5 \times 10^4$ cells/well) were seeded in 96-well plates and incubated overnight. The cells were subsequently exposed to five different concentrations of the DBP mixture (3, 6.25, 12.5, 25, and 50 μM) or 0.5 % DMSO (solvent control) in a serum-free medium for 48 h. In additional experiments, cells were exposed to individual DBPs at a fixed concentration of 5 μM. After exposure, cells were washed with PBS and incubated with 100 μL of a reaction mix containing 5 % AB and 4 μM CFDA-AM for 30 min at 37 °C and 5 % $CO_2$. Then, the emitted fluorescence was measured in a microplate reader (Tecan- Infinite® M Plex, Tecan Trading AG, Switzerland) at the wavelength pairs of 530/590 nm and 485/530 nm for AB and CFDA-AM, respectively. Additionally, the background fluorescence of blanks ($n = 6$), e.g., wells containing serum-free medium with AB and CFDA-AM but devoid of cells, was also measured. The fluorescence values of the treatment groups were adjusted by subtracting the corresponding blank values. Finally, the percentage of cell viability was calculated relative to the fluorescence values of the solvent control. Three independent experiments with six replicates were performed per treatment.

### 2.4. Generation of reactive oxygen species (ROS)

A549 cells ($5 \times 10^4$ cells/well) were seeded in 96-well plates and incubated for 24 h. After washing with PBS (pH 7.4), cells were incubated with 20 μM H2DCF-DA in DPBS supplemented with 10 mM glucose (DPBS-Glu) for 30 min at 37 °C as described in LeBel et al. (1992). Then, the solution was removed, and cells were washed with PBS and exposed to 3–50 μM DBP mixture, 0.1 % and 0.5 % DMSO (solvent controls) or 1 μM SIN-1 (positive control), all diluted in DPBS-Glu. In additional experiments, cells were exposed to individual DBPs at a fixed concentration of 5 μM. The fluorescence of oxidized dichlorofluorescein was measured after 15, 30, 60, and 120 min of exposure in an Infinite® M Plex microplate reader at 485/528 nm. Results were expressed as the fold change over the basal fluorescence measured in cells exposed to the solvent (0.5 % DMSO) (Pérez-Albaladejo et al., 2023). Each experiment was performed in triplicate, with six technical replicates per plate.

### 2.5. Micronuclei frequency

The ability of the DBP mixture to induce genotoxicity was estimated by the frequency of micronuclei in exposed A549 cells, as previously described with some modifications (Schnell et al., 2013). Briefly, A549 cells ($1 \times 10^5$ cells/well) were seeded in 6-well plates containing 3 glass coverslips (Ø 12 mm; Marienfeld, Germany) per well. After a 24 period of attachment, cells were exposed to the DBP mix (50 μM), 0.5 % DMSO (solvent control), or 0.25 μM mitomycin C (positive control) for 48 h. The doubling time of A549 cells under the assay conditions was 34 h. Thus, a 48-hour exposure period was deemed sufficient for the cells to undergo division.

Next, cells were fixed with 4 % formaldehyde, stained with 5 μM bisbenzimide Hoechst 33342, and the coverslips mounted with Vectashield® H-1000 (Vector Laboratories, CA, USA). From each slide, 100 tiff-data images (40× objective) were scanned and merged into a tiled image containing over 2000 cells using the EVOS M7000 Cell Imaging System (Thermo). Celleste 5.0 Image Analysis software was used to automatically count the nuclei in the tiled image. The software performance was validated by manually counting the nuclei in selected tiff-data images. Micronuclei frequency was determined by manually evaluating 2000 nuclei from the tiff-data images. Only micronuclei with round or oval shapes, with a staining intensity similar to the nucleus, and completely separated from the nucleus were counted (Fenech, 2000).

### 2.6. Lipidomic analysis

A549 cells ($3 \times 10^5$ cells/well) were seeded in a 24-well plate and incubated overnight. The cells were then exposed to different concentrations of the DBP mixture (1, 10, and 50 μM) or 0.5 % DMSO (solvent control) in a serum-free medium. Eight replicates (8 wells) were considered for each experimental condition. After 24 h of exposure, the culture medium of each well was collected and kept on ice. The cells were washed with PBS, detached with 0.25 % trypsin, resuspended in PBS, and centrifuged at 2000-g for 15 min at 4 °C. The resulting pellet was collected and stored at −80 °C under an argon atmosphere until extraction. The collected culture medium was centrifuged at 4 °C (2000-g for 10 min) to eliminate any remaining cells. Subsequently, the supernatants underwent two additional rounds of centrifugation at 10,000-g for 30 min, as reported by Xiao et al. (2014). The resulting supernatants, potentially enriched with extracellular vesicles (EVs), were stored at −80 °C until extraction.

Cell pellets were thawed on ice and processed as described in Marqueño et al. (2019). Briefly, ethyl acetate (0.5 mL) was added to the cell pellets, the mixture was vortexed, placed in an ultrasound water bath for 1 min, and further incubated at room temperature for 30 min. The mixture was then centrifuged (2500-g for 10 min at 4 °C), and the supernatant was collected. This process was repeated three times. The supernatants obtained were combined and dried under a gentle stream of nitrogen. The dried extracts were stored at −20 °C in an argon atmosphere until analysis.

The culture medium containing EVs was extracted using ethyl acetate (200 μL of culture medium in 1 mL ethyl acetate). The mixture was shaken (100 rpm) at room temperature for 30 min, centrifuged (2500-*g* for 10 min), and the supernatant was collected. The extraction process was performed three times. The combined supernatants were evaporated under a gentle stream of nitrogen, and the dried extracts were stored at −20 °C under argon until analysis.

Before ultra-high-performance liquid chromatography (UHPLC) – high-resolution mass spectrometry (HRMS) analysis of lipids, dried extracts of cell pellets and culture medium were reconstituted in 300 and 100 μL of methanol, respectively, and the internal standards added at a final concentration of 50 pmol (PC-P, DG, and LPC), 100 pmol (TG and SM), or 200 pmol (PC, CE, Cer, PE, PS, PG, and PI).

UHPLC-HRMS analysis was performed with an Elute UHPLC system coupled with an Impact II quadrupole time-of-flight (QToF) mass spectrometer (Bruker Daltonics, Bremen, Germany). Extracts (10 μL) were injected into an Acquity UPLC BEH C8 column (100 × 2.1 mm, 1.7 μm) (Waters, Ireland) kept at 30 °C. The mobile phases used were (A) water with 2 mM ammonium formate and 0.01 % formic acid, and (B) methanol with 1 mM ammonium formate and 0.01 % formic acid. Lipid separation was conducted at a constant flow rate of 0.25 mL/min with a linear organic gradient: 0–0.6 min 80 % of B, 0.6–3 min B increased to 90 %, 3–6 min 90 % of B, 6–14 min B increased to 99 %, 14–19 min 99 % of B, 19–22 min B decreased to 80 %, 22–25 min 80 % of B. Untargeted mass acquisition was carried out in positive electrospray mode with a capillary voltage of +4500 V and collision energy of 7 eV. The source desolvation temperature was set to 220 °C, the drying gas ($N_2$) flow rate to 10 L/min, and the nebulizer gas ($N_2$) pressure to 4 bar. The mass-to-charge ratio (*m/z*) scan range was 200–1200, and mass spectra were acquired at a rate of 12 Hz in auto MS/MS mode. External and internal mass calibration was based on sodium formate ion clusters.

Data processing was performed with MetaboScape software (v. 2022,

Bruker Daltonics). The extraction of features, capturing important information such as m/z, chromatographic retention time, and intensity, was done using the T-Rex 3D algorithm. Processing parameters for feature extraction included an intensity threshold of >1000 counts to ensure the selection of significant peaks, a minimum peak length of 5 spectra (acquisition points), a mass range of 200 to 1200 m/z, and a retention time range of 2–25 min. The annotation process involved evaluating accurate m/z isotopic patterns and MS/MS spectra based on fragmentation rules specific to lipid classes (Helmer et al., 2021). The precursor ion mass (m/z) tolerance was set to 5 ppm, the isotope pattern match (mSigma) value was set to 250, and the MS/MS match score was set to 400. The lipid species were commonly annotated using a standardized nomenclature, indicating the lipid class followed by the number of carbons and double bond equivalents. For some lipids, HRMS data combined with MS/MS fragmentation provided additional information, such as the fatty acid composition (e.g., PC 16:0_18:0). The resulting list of annotated lipids was exported for further quantification. Cer, LPC, PC, PC-P, PE, PS, SM, and sphingosines (SPB) were identified through their protonated molecular ion $[M + H]^+$; while, CE, DG, PG, PI, and TG were detected through their corresponding ammonium adducts $[M + NH_4]^+$. Quantification of lipid species was performed using their respective internal standard, except for PC-plasmalogen/PC-plasmanyl (PC-P/PC-O) and SPB, for which PC-P and SM standards were used, respectively. The relative standard deviation (RSD) of the signal of each internal standard in the samples throughout the analytical batch was below 10 %, except for PI and PS that presented values of 12 % and 15 %, respectively (Table S2).

### 2.7. Statistical analysis

Statistical analyses were performed using SPSS software v25 (IBM, Chicago, IL, USA). The normal distribution of the data and the homogeneity of the variance were assessed using Shapiro–Wilk and Levene's tests, respectively. Differences between control and exposed groups for ROS and micronuclei formation were evaluated using one-way ANOVA, followed by Tukey's post-hoc test ($P < 0.05$).

The online software Metaboanalyst 5.0 was used to analyze the lipidomic data (Pang et al., 2021). Missing values were imputed by substituting them with 1/5 of the minimal positive value of each variable in the corresponding sample replicates, and data were normalized by auto-scaling. Partial least squares-discriminant analysis (PLS-DA) was used to differentiate between experimental groups. The lipids responsible for differentiation were selected based on their variable importance for the projection (VIP). The quality of the PLS-DA model was evaluated by using the R2 and Q2 values, which measure the ability to predict the internal correct classification in the experiment and the external predictability of the model, respectively.

## 3. Results

Upon exposing A549 cells to a mixture of DBPs at concentrations of up to 25 μM for 48 h, no significant changes in cell viability were observed (Fig. S1). However, a slight decrease in cell viability (7 %) was noted after exposure to 50 μM DBP mix (Fig. S1-A). Following exposure to individual DBPs, marginal decreases in cell viability were observed for TBP and DIAA (10 %; AB and CFDA-AM), and DCBQ (15 %; CFDA-AM) (Fig. S1—B) at 5 μM.

Likewise, concentrations of the DBP mixture up to 12.5 μM did not induce the generation of ROS in A549 cells. However, when cells were exposed to higher concentrations, viz., 25 and 50 μM, increases up to 1.5- and 4-fold in ROS production were observed after 15 min exposure, respectively. This increase in ROS generation persisted throughout the entire 180-min exposure period (Fig. 1-A). When cells were exposed to individual compounds at a fixed concentration of 5 μM, DCBQ induced a 30-fold increase in ROS production after 15 min, while halophenols (TBP, TCP) and DBHB led to a moderate increase in ROS (2- to 2.5-fold).

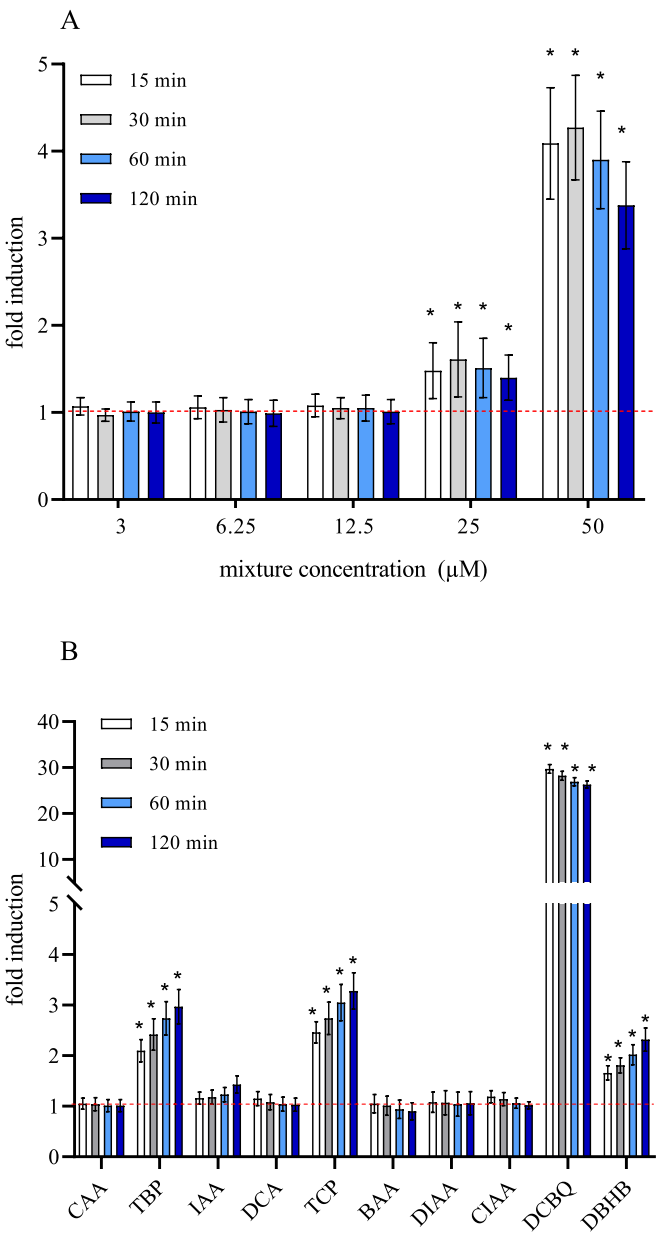


**Fig. 1.** ROS generation in A549 cells in the presence of (A) different concentrations of the DBP mixture; (B) individual DBPs at a concentration of 5 μM. The asterisk indicates significant differences from the solvent control (Tukey test, one-way ANOVA, $p < 0.05$). Data shown as the fold change relative to the solvent control (mean ± SD; $n = 3$ experiments; 6 replicates each). The red dotted line indicates control value.

The other DBPs present in the mixture did not induce ROS when tested individually (Fig. 1-B).

The genotoxicity assessment revealed that the DBP mixture at 50 μM induced the formation of micronuclei (31.7 ± 4.0 ‰) in A549 cells (Fig. S2). The frequencies of micronuclei formation in the positive control (cells exposed to 0.25 μM mitomycin C) and solvent control (cells exposed to 0.5 % DMSO) were 40.3 ± 12.0 ‰ and 7.4 ± 0.6 ‰, respectively.

A comprehensive analysis of the lipidome of A549 cells revealed the presence of about 300 lipids (Table S3). Among them, PCs emerged as the most prevalent lipid species (Fig. S3-A). Specifically, PCs with acyl chains 16:0/16:0, 16:0_16:1, 16:0_18:1, 16:1_18:1, and 18:1_18:1 accounted for 49 % of the total PCs detected (Fig. S4-A). Additionally, significant proportions of TGs and CEs were identified, comprising 16 %

and 12 % of the total lipids, respectively (Fig. S3-A). The dominant TG species, enriched in FAs 16:0_16:1_18:1, 16:0_18:1_18:1, 16:1_18:1_18:1, 16:1_18:1_20:1, represented 34.5 % of the total TGs observed (Fig. S4—B). The most abundant CE species were CE 18:1 and CE 22:6, accounting for 55.5 % of the total CEs detected (Fig. S4—C).

The lipidomic analysis of the culture medium, potentially enriched with extracellular vesicles, identified 93 lipids (Table S4), with a significant enrichment of CEs followed by PCs, sphingolipids (SM, SPB, and Cer), and PEs (Fig. S3—B). The most abundant CEs were CE 18:1, 18:2, 20:4. Among PCs, PC 16:0_18:1 and PC 18:0_18:1 were the predominant species, making up approximately 43 % of the total PCs. Furthermore, SM 18:1;O2/16:0 and SM 18:1;O2/24:1 represented about 57 % of the total SMs (Fig. S5A–C).

When A549 cells were exposed to the mixture of 10 DBPs at concentrations of 1 and 10 μM (0.1 and 1 μM the individual components, respectively), no major changes in the relative abundance of the different lipid classes were observed (Fig. 2). Also, PLS-DA evidenced poor separation among exposed and control cells (Fig. S6). Conversely, exposure to a concentration of 50 μM of the mixture of DBPs (5 μM for each component) resulted in a significant accumulation of TGs. Furthermore, an increase of CEs, PC-P/PC-Os, and SPBs, and a decrease of DGs and Cer was observed with increasing exposure concentration of the DBP mixture (Figs. 2 and S7A–B). This contrasts with the results obtained in the lipidomic analysis of the culture medium, which evidenced an increase in the overall abundance of CEs, LPCs, PCs, PC-P/PC-Os, PEs, and SMs at the lowest concentration tested (1 μM of mixture); while no significant changes were observed at concentrations of 10 and 50 μM. Interestingly, the levels of sphingosine-based lipids, including SPBs and Cers, remained relatively stable across all tested concentrations (Fig. 3).

The multivariate PLS-DA analysis revealed a clear differentiation between the lipidome of control cells and cells exposed to 50 μM of the DPB mixture (Fig. 4). The covariance explained by two components was 68.5 % (R2 = 0.95 and Q2 = 0.88); and 126 lipids had VIP scores higher than 1 (Table S5). Among them, it was detected an up-regulation of TGs, many of them containing FA 18:1 (16:0_16:1_18:1, 16:0_18:1_18:1, 16:0_18:0_18:1, 16:0_18:1_20:1, 16:1_18:1_18:1, 16:1_18:1_20:1, and 18:1_18:1_20:1), and a concomitant decrease in DGs (16:0_26:0 and 44:1) (Fig. 4). Additionally, the volcano plot unveiled identical findings, showing an accumulation of TGs and a decrease of DGs and PCs (18:1_26:1, 42:0, 42:1, and 44:1) in exposed cells (Fig. S8).

## 4. Discussion

This study assessed the toxic, genotoxic, and lipidomic alterations resulting from the acute exposure of human alveolar A549 cells to a mixture of selected DBPs, including IAA, BAA, CAA, DCAA, CIAA, DIAA, DCBQ, TCP, TBP, and DBHB. The exposure concentration range 1–50 μM for the DBP mixture (with a maximum of 5 μM of each DBP) had no strong effects on cell viability after 48 h. Only the highest tested concentration (50 μM) resulted in ~7 % reduction of cell viability. This effect was mainly driven by TBP, DIAA, and DCBQ. In a previous study, we found that IAA and BAA showed cytotoxicity in JEG-3 placental cells at a concentration of 5 μM after 24-hour exposure ($EC_{10}$: 3.5 ± 0.2 μM for IAA, and $EC_{10}$: 12.5 ± 1.8 μM for BAA), while CAA, CIAA, and DIAA were not cytotoxic at the highest tested concentration (500 μM) (Pérez-Albaladejo et al., 2023). IAA also emerged as the most toxic compound for CHO cells, inducing a toxic response at a concentration as low as 0.5 μM after 72 h exposure, followed by BAA (2 μM), TBAA (5 μM), and DIAA (100 μM) (Richardson et al., 2008; Plewa et al., 2010). Regarding halophenols, TCP and TBP exhibited no cytotoxic effects in JEG-3 cells at concentrations below 300 and 500 μM, respectively, while DCBQ ($EC_{50}$: 28.6 ± 2.8 μM) and DBHB ($EC_{50}$: 26.0 ± 2.7 μM) showed significant toxicity (Pérez-Albaladejo et al., 2024). The small discrepancies among studies suggest that, beyond experimental factors like exposure time, variation in sensitivity may be attributed to the distinct responses exhibited by the different cell lines.

On the contrary, other studies have reported the toxicity of individual DBPs at concentrations much higher than the ones tested in our study. For instance, $EC_{50}$s of BAA, CAA, and DCAA were 10, 810, and 7300 μM, respectively in CHO AS52 cells (Plewa et al., 2010). $EC_{50}$s of CAA, BAA, IAA, and BDBQ ranged from 34 to 1200 μM in Caco-2 cells, (Procházka et al., 2015). Hall et al. (2020) reported $EC_{50}$ values below 50 μM for IAA and BAA, while CAA had an $EC_{50}$ value of 100 μM in human breast adenocarcinoma cells (MCF7). Although some discrepancies have been detected among studies depending on the cell type and exposure time, it is evident that the highest exposure concentration used in the present study (50 μM mixture, 5 μM of each DBP) is below all previously reported $EC_{50}$ values, and it only induced marginal cytotoxicity in A549 cells.

Interestingly, ROS production in A549 cells was stimulated by 3.5-fold at the highest concentration of the DBP mixture (50 μM). The predominant drivers of ROS generation were DCBQ (30-fold induction), along with halophenols and DBHB (2 to 2.5-fold), indicating an additive effect of the components in the mixture. Previous studies have demonstrated the oxidative potential of some individual DBPs, particularly HBQs (up to 80-fold) and haloacetonitriles (Hassoun and Ray, 2003; Du et al., 2013; Li et al., 2023; Pérez-Albaladejo et al., 2024). Consistent with our findings, trihalophenols (TBP, TCP) led to an increase of up to 2.5-fold in the formation of ROS in human placenta JEG-3 cells (Pérez-Albaladejo et al., 2024) and a 4-fold increase in HepG2 cells (Li et al., 2023). The reduction of cellular glutathione, a crucial antioxidant,

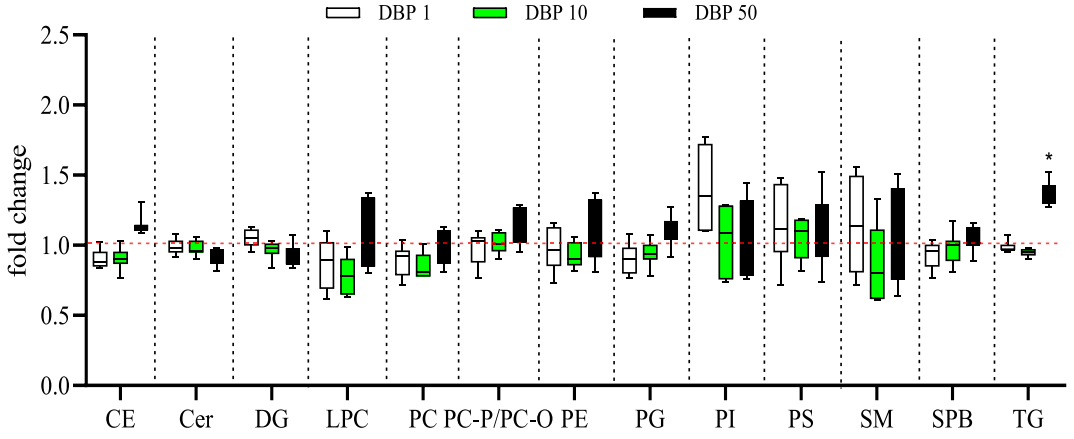


**Fig. 2.** Lipidomic alteration in A549 cells exposed to 1, 10, and 50 μM of the DBP mixture. Data are presented as a fold-change over solvent control (mean ± S.D.; $n = 8$). The red dotted line indicates control value. The asterisk indicates significant differences from the solvent control (Tukey test, one-way ANOVA, $p < 0.05$).

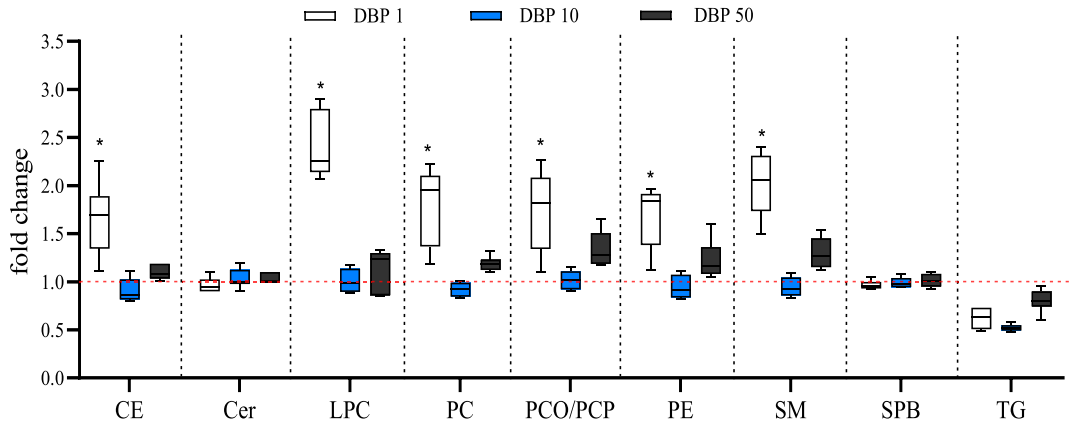


**Fig. 3.** Lipid class variations observed in the culture medium/extracellular vesicles of cells exposed to different concentrations (1, 10, and 50 μM) of the DBP mixture. The data are presented as the fold-change relative to the solvent control (mean ± S.D.; $n = 6$). The control value is represented by a red dotted line. The asterisks indicate statistically significant differences compared to the solvent control group (Tukey test, one-way ANOVA, $p < 0.05$).

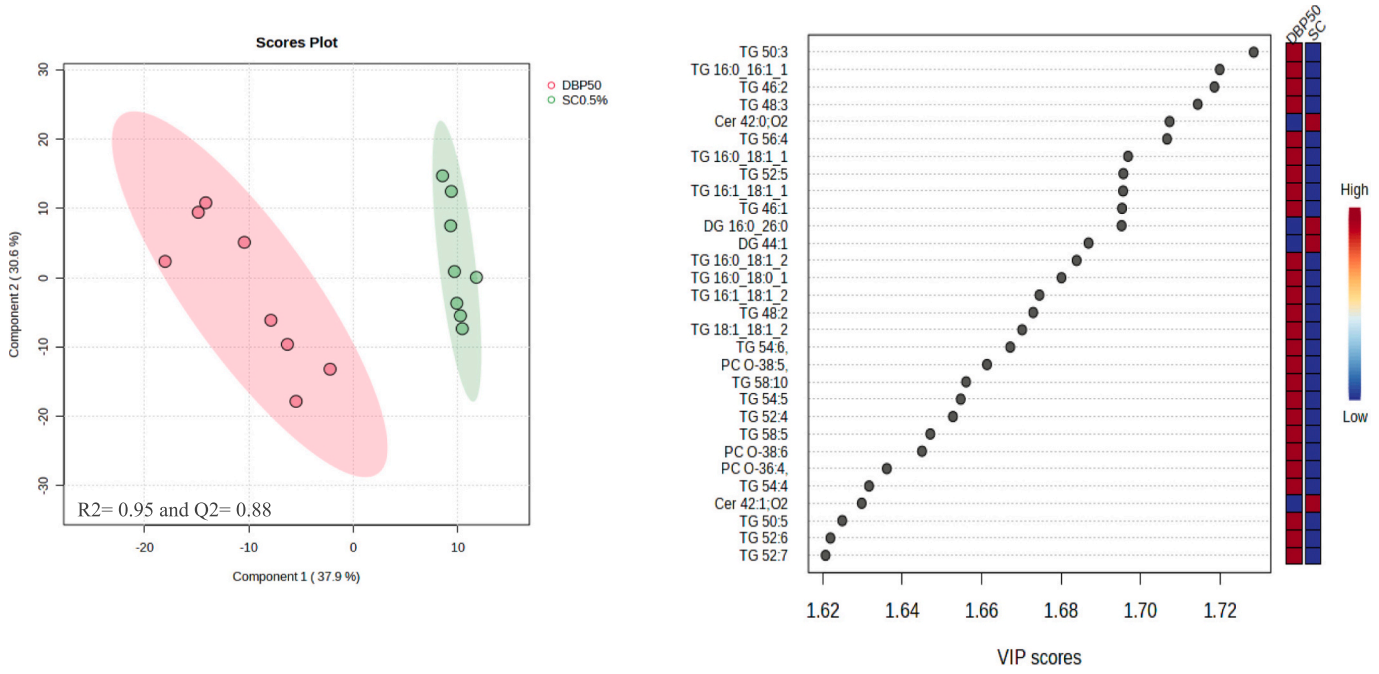


**Fig. 4.** PLS-DA scores plot shows the discrimination between the cells exposed to 50 μM of the DBP mixture and the solvent control. VIP score plot shows the top 30 most important lipid species identified by PLS-DA. Heatmap indicates the up-regulation (red) and down-regulation (blue) of the specific lipids in solvent control (SC) and exposed cells.

might be a mechanism through which 3-MX and haloacetonitriles, such as dibromo- and dichloro-acetonitrile contribute to oxidative stress (Yuan et al., 2006; Li et al., 2022). DBPs could also activate the nuclear factor erythroid 2-related factor 2 (Nrf2) signaling pathway in HT22 cells and HepG2 cells, which is a key regulator of cellular defense against oxidative stress injury (Wang et al., 2013; Li et al., 2022).

The increase of ROS levels by DBP exposure might potentially lead to oxidative stress, and result in nucleic acid damage (Cemeli et al., 2006; Yuan et al., 2006; Du et al., 2013). Previous studies have linked the genotoxicity of mono-HAAs to oxidative stress (Cemeli et al., 2006; Ali et al., 2014). Additionally, exposure to four HBQs at concentrations ranging from 25 to 125 μM, resulted in increased levels of hydroxydeoxyguanosine (8-OHdG), a biomarker of oxidative damage, and increased generation of ROS in T24 bladder cancer cells (Du et al., 2013). Interestingly, exposure to 50 μM of the DBP mixture resulted in approximately a two-fold increase in the formation of micronuclei in A549 cells. This genotoxic effect was mainly driven by the presence of IAA, BAA, and DCBQ in the mixture (Pérez-Albaladejo et al., 2023, 2024). Similarly, exposure to IAA, BAA, and CAA at concentrations of 22 μM, 57 μM, and 3.42 mM, respectively, induced DNA damage in the human small intestine epithelial cell line FHs 74 (Attene-Ramos et al., 2010). In a study by Kogevinas et al. (2010) the frequencies of micronuclei formation in lymphocytes and urothelial cells showed a non-significant increase among swimmers. These findings underscore the importance of further research to better understand and mitigate the potential genotoxic and DNA-damaging effects of these compounds in various contexts, including environmental and occupational exposures.

Apart from the ability of the mixture to generate ROS and induce potential genotoxic effects, significant alterations were observed in the lipidome of A549 lung cells. Cells exposed to 10 and 50 μM DBP mixture showed increased levels of PC-P/PC-Os. Furthermore, at the highest concentration tested (50 μM), an additional increase in TGs and CEs was observed, coupled with a simultaneous decrease of PCs and DGs (Fig. S8). PC-P/PC-Os may play a key role in the organization and

stability of lipid raft microdomains, e.g., cholesterol-rich membrane regions involved in cell signaling, but also a subset of these lipids (PC-Ps) may function as endogenous antioxidants, neutralizing free radicals and preventing oxidative damage (Dean and Lodhi, 2018). Thus, the observed increase in PC-P/PC-Os might be interpreted as a cellular defense mechanism against the ROS generated by DBPs, but also a restructuring of plasma membranes due to exposure. Additionally, several studies have demonstrated that elevated levels of ether lipids in cancer cells are often associated with increased pathogenicity (Benjamin et al., 2013).

The accumulation of neutral lipids, TGs and CEs, associated with lipid storage and the formation of lipid droplets within the cells, was particularly pronounced in lung cells exposed to the highest concentration of the DBP mixture (50 μM). In contrast, PCs and DGs were markedly reduced (Fig. S8). The upregulation of intracellular TGs and CEs has been related to endoplasmic reticulum (ER) stress and the progression of hepatic steatosis, as well as various pathophysiological conditions (Cao and Kaufman, 2014; Werstuck et al., 2001). However, to the best of our knowledge, this is the first reported case of such upregulation occurring in lung cells after exposure to DBPs. The increase in TGs combined with the decrease in DGs supports an increase in diacylglycerol acyltransferase (DGAT) activity (Coleman, 2004). Moreover, the hydrolysis of PCs may have resulted in the release of fatty acids, which can be utilized in the synthesis of TGs (Testerink et al., 2009). Extensive lipid deposition has been detected in the lungs of animals with type 2 diabetes mellitus, along with other abnormalities that can impair lung mechanics and alveolar gas exchange (Foster et al., 2010). Romero et al. (2014) showed that chronic alcohol ingestion induces lipid synthesis in the lungs, leading to a lung phenotype characterized by a marked accumulation of TGs.

Furthermore, given the presence of PCs on the surface of lipid droplets, particularly in proximity to TGs, alterations in the PCs content can impact the dynamics of lipid droplets by influencing the PCs to TGs ratio (Guo et al., 2008). Thus, a decrease in PC biosynthesis during the increased TG accumulation results in the formation of larger lipid droplets, which enhances the overaccumulation of lipid droplets in the tissue (Krahmer et al., 2011; Listenberger et al., 2018; Wu et al., 2022). Moreover, the reduction of PCs induced by a mixture of DBP in lung cells may have an impact on the composition of lung surfactants, which are a complex mixture of phospholipids, mainly PCs and proteins, with a vital role in maintaining optimal respiratory function (Ishiguro et al., 2008). Thereby, an alteration of the phospholipid content of lung surfactants will alter normal hemostasis and function, causing respiratory problems (Rodríguez-Capote et al., 2006; Schmidt et al., 2002; Whitsett et al., 2015).

Regarding the culture medium, its lipid composition exhibited enrichment in CEs followed by PCs, sphingolipids (CMs, SPBs, and Cers), and PEs. In particular, some specific lipids, such as CE 20:4, SM18:1_16:0, SM 18:1_24:1, LPC 16:0, PC 16:0/16:0, PC16:0_20:4, PC 16:0_22:5, PC 16:0_22:6, PC 18:0_18:1, PC 34:2, and PC 36:3 have previously been proposed as markers of lung cancer in exosomes and were attributed to the release of EVs by lung cancer cells (Hsu et al., 2022). EVs secreted by various cell types have a role in intercellular communication by transferring bioactive molecules, including proteins, nucleic acids, and lipids, between cells (Mohan et al., 2020). Interestingly, exposure of A549 cells to 1 and 50 μM DBP mixture elevated the concentration of some of these lipid markers including CE 20:4, SM 18:1_16:0, SM 18:1_24:1, PC 18:0_18:1, and PC 34:2 (Fig. S9B–F).

Surprisingly, the lowest concentration of the DBP mixture (1 μM) had a pronounced effect on the lipid content of EV enriched culture medium when compared to concentrations of 10 μM and 50 μM. The lowest concentration of DBPs resulted in a notable increase in the level of CEs, PCs, LPC, and SMs in the culture medium. Based on the available research on the influence of cholesterol on exosome release (Abdullah et al., 2021), it is reasonable to hypothesize that the alteration of cellular CE levels caused by DBPs can influence the release of EVs from the cells (Abdullah et al., 2021). In our study, the lowest concentration of DBPs leads to decreased levels of CEs in the cells (as depicted in Fig. S7-A), and possibly, increased EV release from the cells. Recent studies have revealed that changes in lipid mediators present in airway EVs may play a role in the development and persistence of chronic airway inflammation (Hough et al., 2018). This suggests the need to further investigate alterations in the EV lipidome, particularly considering the already established relationship between various disorders, such as atherosclerosis, cancer, non-alcoholic fatty liver disease (NAFLD), obesity, and Alzheimer's disease, and the dysregulation of lipid metabolism and altered exosome-mediated lipid communication (Wang et al., 2020). Thus, considering this evidence and our findings, we believe that chronic exposure to DBPs, at concentrations close to 50 μM (mixture concentration), but far below the $EC_{50}$ for cytotoxicity, might increase the incidence of lung diseases. These could include conditions associated with impaired pulmonary function and immunity, as indicated by the chronic endoplasmic reticulum (ER) stress situation (Romero et al., 2014).

Overall, this study uncovers the potential health risks associated with exposure to complex mixtures of DBPs even at non-toxic concentrations. Although, it considers a mixture of ten DBPs, which is a very small fraction of the DBP mixtures present in disinfected waters, the selected mixture induced the generation of ROS, and led to DNA damage and significant changes in the lipid profile of lung cells. Such effects, namely increased concentrations of TGs, CEs and PC-P/PC-Os in cells, may have been associated with an increased risk of respiratory problems, such as asthma. The DBP concentrations that produced effects in this study were one to three orders of magnitude higher (depending on the compound) than those typically measured in drinking water (~20 times in the case of DCAA). However, DBP levels and hence DBP exposure are notably increased in certain environments, such as indoor swimming pools or chlorine-based cleaning facilities, where individual DBP levels in water may be similar to those tested in this study, or even higher for some of them. In such scenarios, inhalation of polar low-volatile DBPs may be a relevant exposure pathway; however, there is not sufficient information on the levels of emerging and low-volatile DBPs in the gas phase of these environments. The application of the lipidomic approach to assessing the mixture toxicity can help to enhance our understanding of the molecular mechanisms involved in DBP toxicity at the respiratory level, identify potential biomarkers, and shed light on the functional consequences of DBP exposure.

## CRediT authorship contribution statement

**Mahboubeh Hosseinzadeh:** Data curation, Investigation, Methodology, Writing – original draft, Writing – review & editing, Formal analysis. **Cristina Postigo:** Conceptualization, Writing – review & editing. **Cinta Porte:** Conceptualization, Methodology, Supervision, Writing – review & editing, Funding acquisition.

## Declaration of competing interest

The authors declare that they have no known competing financial interests or personal relationships that could have appeared to influence the work reported in this paper.

## Data availability

Data will be made available on request.

## Acknowledgments

This work was supported by projects PID2021-122592NB-I00 and CEX2018-000794-S (Ministerio de Ciencia e Innovación). CP acknowledges the ComFuturo Programme (2nd edition) funded by the Fundación General del CSIC and grant RYC2020-028901-I funded by

MCIN/AEI/10.13039/501100011033 and "ESF investing in your future".

## Appendix A. Supplementary data

Supplementary data to this article can be found online at https://doi.org/10.1016/j.scitotenv.2024.170331.

## References


Abdullah, M., Nakamura, T., Ferdous, T., Gao, Y., Chen, Y., Zou, K., Michikawa, M., 2021. Cholesterol regulates exosome release in cultured astrocytes. Front. Immunol. 12, 722581 https://doi.org/10.3389/fimmu.2021.722581.

Agudelo, C.W., Samaha, G., Garcia-Arcos, I., 2020. Alveolar lipids in pulmonary disease. A review. Lipids Health Dis 19, 122. https://doi.org/10.1186/s12944-020-01278-8.

Ali, A., Kurzawa-Zegota, M., Najafzadeh, M., Gopalan, R.C., Plewa, M.J., Anderson, D., 2014. Effect of drinking water disinfection by-products in human peripheral blood lymphocytes and sperm. Mutation Research/Fundamental and Molecular Mechanisms of Mutagenesis 770, 136–143. https://doi.org/10.1016/j.mrfmmm.2014.08.003.

Attene-Ramos, M.S., Wagner, E.D., Plewa, M.J., 2010. Comparative human cell Toxicogenomic analysis of Monohaloacetic acid drinking water disinfection byproducts. Environ. Sci. Technol. 44, 7206–7212. https://doi.org/10.1021/es1000193.

Benjamin, D.I., Cozzo, A., Ji, X., Roberts, L.S., Louie, S.M., Mulvihill, M.M., Luo, K., Nomura, D.K., 2013. Ether lipid generating enzyme AGPS alters the balance of structural and signaling lipids to fuel cancer pathogenicity. Proc. Natl. Acad. Sci. U. S. A. 110, 14912–14917. https://doi.org/10.1073/pnas.1310894110.

Cantor, K.P., Villanueva, C.M., Silverman, D.T., Figueroa, J.D., Real, F.X., Garcia-Closas, M., Malats, N., Chanock, S., Yeager, M., Tardon, A., Garcia-Closas, R., Serra, C., Carrato, A., Castaño-Vinyals, G., Samanic, C., Rothman, N., Kogevinas, M., 2010. Polymorphisms in *GSTT1*, *GSTZ1*, and *CYP2E1*, Disinfection By-products, and Risk of Bladder Cancer in Spain. Environ. Health Perspect. 118, 1545–1550. doi:https://doi.org/10.1289/ehp.1002206.

Cao, S.S., Kaufman, R.J., 2014. Endoplasmic reticulum stress and oxidative stress in cell fate decision and human disease. Antioxid. Redox Signal. 21, 396–413. https://doi.org/10.1089/ars.2014.5851.

Cardador, M.J., Gallego, M., 2011. Haloacetic acids in swimming pools: swimmer and worker exposure. Environ. Sci. Technol. 45, 5783–5790. https://doi.org/10.1021/es103959d.

Cemeli, E., Wagner, E.D., Anderson, D., Richardson, S.D., Plewa, M.J., 2006. Modulation of the cytotoxicity and genotoxicity of the drinking water disinfection byproduct Iodoacetic acid by suppressors of oxidative stress. Environ. Sci. Technol. 40, 1878–1883. https://doi.org/10.1021/es051602r.

Chen, Y.-H., Qin, L.-T., Mo, L.-Y., Zhao, D.-N., Zeng, H.-H., Liang, Y.-P., 2019. Synergetic effects of novel aromatic brominated and chlorinated disinfection byproducts on Vibrio qinghaiensis sp.-Q67. Environ. Pollut. 250, 375–385. https://doi.org/10.1016/j.envpol.2019.04.009.

Chowdhury, S., 2013. Exposure assessment for trihalomethanes in municipal drinking water and risk reduction strategy. Sci. Total Environ. 463–464, 922–930. https://doi.org/10.1016/j.scitotenv.2013.06.104.

Chu, T.-S., Cheng, S.-F., Wang, G.-S., Tsai, S.-W., 2013. Occupational exposures of airborne trichloramine at indoor swimming pools in Taipei. Sci. Total Environ. 461–462, 317–322. https://doi.org/10.1016/j.scitotenv.2013.05.012.

Coleman, R., 2004. Enzymes of triacylglycerol synthesis and their regulation. Prog. Lipid Res. 43, 134–176. https://doi.org/10.1016/S0163-7827(03)00051-1.

Dean, J.M., Lodhi, I.J., 2018. Structural and functional roles of ether lipids. Protein Cell 9, 196–206. https://doi.org/10.1007/s13238-017-0423-5.

Du, H., Li, J., Moe, B., McGuigan, C.F., Shen, S., Li, X.-F., 2013. Cytotoxicity and oxidative damage induced by Halobenzoquinones to T24 bladder Cancer cells. Environ. Sci. Technol. 47, 2823–2830. https://doi.org/10.1021/es303762p.

European Commission, 2020. Directive (EU) 2020/2184 of the European Parliament and of the council of 16 December 2020 on the quality of water intended for human consumption (recast) (text with EEA relevance). http://data.europa.eu/eli/dir/2020/2184/oj.

Fenech, M., 2000. The in vitro micronucleus technique. Mutation Research/Fundamental and Molecular Mechanisms of Mutagenesis 455, 81–95. https://doi.org/10.1016/S0027-5107(00)00065-8.

Font-Ribera, L., Kogevinas, M., Zock, J.-P., Gómez, F.P., Barreiro, E., Nieuwenhuijsen, M. J., Fernandez, P., Lourencetti, C., Pérez-Olabarría, M., Bustamante, M., Marcos, R., Grimalt, J.O., Villanueva, C.M., 2010. Short-term changes in respiratory biomarkers after swimming in a chlorinated Pool. Environ. Health Perspect. 118, 1538–1544. https://doi.org/10.1289/ehp.1001961.

Font-Ribera, L., Marco, E., Grimalt, J.O., Pastor, S., Marcos, R., Abramsson-Zetterberg, L., Pedersen, M., Grummt, T., Junek, R., Barreiro, E., Heederik, D., Spithoven, J., Critelli, R., Naccarati, A., Schmalz, C., Zwiener, C., Liu, J., Zhang, X., Mitch, W., Gracia-Lavedan, E., Arjona, L., De Bont, J., Tarès, L., Vineis, P., Kogevinas, M., Villanueva, C.M., 2019. Exposure to disinfection by-products in swimming pools and biomarkers of genotoxicity and respiratory damage – the PISCINA2 study. Environ. Int. 131, 104988 https://doi.org/10.1016/j.envint.2019.104988.

Fornander, L., Ghafouri, B., Lindahl, M., Graff, P., 2013. Airway irritation among indoor swimming pool personnel: trichloramine exposure, exhaled NO and protein profiling of nasal lavage fluids. Int. Arch. Occup. Environ. Health 86, 571–580. https://doi.org/10.1007/s00420-012-0790-4.

Foster, D.J., Ravikumar, P., Bellotto, D.J., Unger, R.H., Hsia, C.C.W., 2010. Fatty diabetic lung: altered alveolar structure and surfactant protein expression. American Journal of Physiology-Lung Cellular and Molecular Physiology 298, L392–L403. https://doi.org/10.1152/ajplung.00041.2009.

Goodman, M., Hays, S., 2008. Asthma and swimming: a Meta-analysis. J. Asthma 45, 639–647. https://doi.org/10.1080/02770900802165980.

Guo, Y., Walther, T.C., Rao, M., Stuurman, N., Goshima, G., Terayama, K., Wong, J.S., Vale, R.D., Walter, P., Farese, R.V., 2008. Functional genomic screen reveals genes involved in lipid-droplet formation and utilization. Nature 453, 657–661. https://doi.org/10.1038/nature06928.

Hall, D.R., Yeung, K., Peng, H., 2020. Monohaloacetic acids and Monohaloacetamides attack distinct cellular proteome thiols. Environ. Sci. Technol. 54, 15191–15201. https://doi.org/10.1021/acs.est.0c03144.

Han, J., Zhang, X., Jiang, J., Li, W., 2021. How much of the Total organic halogen and developmental toxicity of chlorinated drinking water might be attributed to aromatic halogenated DBPs? Environ. Sci. Technol. 55, 5906–5916. https://doi.org/10.1021/acs.est.0c08565.

Hassoun, E.A., Ray, S., 2003. The induction of oxidative stress and cellular death by the drinking water disinfection by-products, dichloroacetate and trichloroacetate in J774.A1 cells. Comp. Biochem. Physiol., Part C: Toxicol. Pharmacol. 135, 119–128. https://doi.org/10.1016/S1532-0456(03)00082-6.

Helmer, P.O., Nordhorn, I.D., Korf, A., Behrens, A., Buchholz, R., Zubeil, F., Karst, U., Hayen, H., 2021. Complementing matrix-assisted laser desorption ionization-mass spectrometry imaging with chromatography data for improved assignment of isobaric and isomeric phospholipids utilizing trapped ion mobility-mass spectrometry. Anal. Chem. 93, 2135–2143. https://doi.org/10.1021/acs.analchem.0c03942.

Hough, K.P., Wilson, L.S., Trevor, J.L., Strenkowski, J.G., Maina, N., Kim, Y.-I., Spell, M. L., Wang, Y., Chanda, D., Dager, J.R., Sharma, N.S., Curtiss, M., Antony, V.B., Dransfield, M.T., Chaplin, D.D., Steele, C., Barnes, S., Duncan, S.R., Prasain, J.K., Thannickal, V.J., Deshane, J.S., 2018. Unique lipid signatures of extracellular vesicles from the Airways of Asthmatics. Sci. Rep. 8, 10340. https://doi.org/10.1038/s41598-018-28655-9.

Hrudey, S.E., 2009. Chlorination disinfection by-products, public health risk tradeoffs and me. Water Res. 43, 2057–2092. https://doi.org/10.1016/j.watres.2009.02.011.

Hsu, M.-T., Wang, Y.-K., Tseng, Y.J., 2022. Exosomal proteins and lipids as potential biomarkers for lung Cancer diagnosis, prognosis, and treatment. Cancers 14, 732. https://doi.org/10.3390/cancers14030732.

Hu, Y., Qian, Y., Chen, Y., Guo, J., Song, J., An, D., 2021. Characteristics of trihalomethane and haloacetic acid precursors in filter backwash and sedimentation sludge waters during drinking water treatment. Sci. Total Environ. 775, 145952 https://doi.org/10.1016/j.scitotenv.2021.145952.

Ishiguro, N., Oyabu, M., Sato, T., Maeda, T., Minami, H., Tamai, I., 2008. Decreased biosynthesis of lung surfactant constituent phosphatidylcholine due to inhibition of choline transporter by Gefitinib in lung alveolar cells. Pharm. Res. 25, 417–427. https://doi.org/10.1007/s11095-007-9362-9.

Jeong, C.H., Wagner, E.D., Siebert, V.R., Anduri, S., Richardson, S.D., Daiber, E.J., McKague, A.B., Kogevinas, M., Villanueva, C.M., Goslan, E.H., Luo, W., Isabelle, L. M., Pankow, J.F., Grazuleviciene, R., Cordier, S., Edwards, S.C., Righi, E., Nieuwenhuijsen, M.J., Plewa, M.J., 2012. Occurrence and toxicity of disinfection byproducts in European drinking waters in relation with the HIWATE epidemiology study. Environ. Sci. Technol. 46, 12120–12128. https://doi.org/10.1021/es3024226.

Kargaki, S., Iakovides, M., Stephanou, E.G., 2020. Study of the occurrence and multi-pathway health risk assessment of regulated and unregulated disinfection by-products in drinking and swimming pool waters of Mediterranean cities. Sci. Total Environ. 739, 139890 https://doi.org/10.1016/j.scitotenv.2020.139890.

Kogevinas, M., Villanueva, C.M., Font-Ribera, L., Liviac, D., Bustamante, M., Espinoza, F., Nieuwenhuijsen, M.J., Espinosa, A., Fernandez, P., DeMarini, D.M., Grimalt, J.O., Grummt, T., Marcos, R., 2010. Genotoxic effects in swimmers exposed to disinfection by-products in indoor swimming pools. Environ. Health Perspect. 118, 1531–1537. https://doi.org/10.1289/ehp.1001959.

Kosaka, K., Nakai, T., Hishida, Y., Asami, M., Ohkubo, K., Akiba, M., 2017. Formation of 2,6-dichloro-1,4-benzoquinone from aromatic compounds after chlorination. Water Res. 110, 48–55. https://doi.org/10.1016/j.watres.2016.12.005.

Krahmer, N., Guo, Y., Wilfling, F., Hilger, M., Lingrell, S., Heger, K., Newman, H.W., Schmidt-Supprian, M., Vance, D.E., Mann, M., Farese, R.V., Walther, T.C., 2011. Phosphatidylcholine Synthesis for Lipid Droplet Expansion Is Mediated by Localized Activation of CTP:Phosphocholine Cytidylyltransferase. Cell Metab. 14, 504–515. doi:https://doi.org/10.1016/j.cmet.2011.07.013.

LeBel, C.P., Ischiropoulos, H., Bondy, S.C., 1992. Evaluation of the probe 2′,7′-dichlorofluorescin as an indicator of reactive oxygen species formation and oxidative stress. Chem. Res. Toxicol. 5, 227–231. https://doi.org/10.1021/tx00026a012.

Li, F., Zhou, J., Zhu, X., Lu, R., Ye, Y., Wang, S., Xing, G., Shen, H., 2022. Oxidative injury induced by drinking water disinfection by-products dibromoacetonitrile and dichloroacetonitrile in mouse hippocampal neuronal cells: the protective effect of N-acetyl-L-cysteine. Toxicol. Lett. 365, 61–73. https://doi.org/10.1016/j.toxlet.2022.06.005.

Li, J., Wang, W., Moe, B., Wang, H., Li, X.-F., 2015. Chemical and toxicological characterization of Halobenzoquinones, an emerging class of disinfection byproducts. Chem. Res. Toxicol. 28, 306–318. https://doi.org/10.1021/tx500494r.

Li, X., Gao, X., Li, A., Xu, S., Zhou, Q., Zhang, L., Pan, Y., Shi, W., Song, M., Shi, P., 2023. Comparative cytotoxicity, endocrine-disrupting effects, oxidative stress of halophenolic disinfection byproducts and the underlying molecular mechanisms

revealed by transcriptome analysis. Water Res. 229, 119458 https://doi.org/10.1016/j.watres.2022.119458.
Li, X.-F., Mitch, W.A., 2018. Drinking water disinfection byproducts (DBPs) and human health effects: multidisciplinary challenges and opportunities. Environ. Sci. Technol. 52, 1681–1689. https://doi.org/10.1021/acs.est.7b05440.
Listenberger, L., Townsend, E., Rickertsen, C., Hains, A., Brown, E., Inwards, E., Stoeckman, A., Matis, M., Sampathkumar, R., Osna, N., Kharbanda, K., 2018. Decreasing phosphatidylcholine on the surface of the lipid droplet correlates with altered protein binding and steatosis. Cells 7, 230. https://doi.org/10.3390/cells7120230.
Liu, J., Gibb, M., Pradhan, S.H., Sayes, C.M., 2022. Synergistic cytotoxicity of bromoacetic acid and three emerging bromophenolic disinfection byproducts against human intestinal and neuronal cells. Chemosphere 287, 131794. https://doi.org/10.1016/j.chemosphere.2021.131794.
Llana-Belloch, S., Priego Quesada, J.I., Pérez-Soriano, P., Lucas-Cuevas, Á.G., Salvador-Pascual, A., Olaso-González, G., Moliner-Martinez, Y., Verdú-Andres, J., Campins-Falco, P., Gómez-Cabrera, M.C., 2016. Disinfection by-products effect on swimmers oxidative stress and respiratory damage. Eur. J. Sport Sci. 16, 609–617. https://doi.org/10.1080/17461391.2015.1080306.
Lou, J., Wang, W., Lu, H., Wang, L., Zhu, L., 2021. Increased disinfection byproducts in the air resulting from intensified disinfection during the COVID-19 pandemic. J. Hazard. Mater. 418, 126249 https://doi.org/10.1016/j.jhazmat.2021.126249.
Lu, G., Qin, D., Wang, Y., Liu, J., Chen, W., 2018. Single and combined effects of selected haloacetonitriles in a human-derived hepatoma line. Ecotoxicol. Environ. Saf. 163, 417–426. https://doi.org/10.1016/j.ecoenv.2018.07.104.
Marqueño, A., Pérez-Albaladejo, E., Flores, C., Moyano, E., Porte, C., 2019. Toxic effects of bisphenol a diglycidyl ether and derivatives in human placental cells. Environ. Pollut. 244, 513–521. https://doi.org/10.1016/j.envpol.2018.10.045.
Miao, T., Li, M., Shao, T., Jiang, X., Jiang, L., Zhou, Q., Pan, Y., Wang, Y., Qiu, J., 2022. The involvement of branched-chain amino acids (BCAAs) in aromatic trihalogenated DBP exposure-induced kidney damage in mice. Chemosphere 305, 135351. https://doi.org/10.1016/j.chemosphere.2022.135351.
Mohan, A., Agarwal, S., Clauss, M., Britt, N.S., Dhillon, N.K., 2020. Extracellular vesicles: novel communicators in lung diseases. Respir. Res. 21, 175. https://doi.org/10.1186/s12931-020-01423-y.
Nuckols, J.R., Ashley, D.L., Lyu, C., Gordon, S.M., Hinckley, A.F., Singer, P., 2005. Influence of tap water quality and household water use activities on indoor air and internal dose levels of Trihalomethanes. Environ. Health Perspect. 113, 863–870. https://doi.org/10.1289/ehp.7141.
Pang, Z., Chong, J., Zhou, G., de Lima Morais, D.A., Chang, L., Barrette, M., Gauthier, C., Jacques, P.-É., Li, S., Xia, J., 2021. MetaboAnalyst 5.0: narrowing the gap between raw spectra and functional insights. Nucleic Acids Res. 49, W388–W396. https://doi.org/10.1093/nar/gkab382.
Pedersen, L., Lund, T.K., Mølgaard, E., Kharitonov, S.A., Barnes, P.J., Backer, V., 2009. The acute effect of swimming on airway inflammation in adolescent elite swimmers. J. Allergy Clin. Immunol. 123, 502–504. https://doi.org/10.1016/j.jaci.2008.11.039.
Pereira, M.A., Li, K., Kramer, P.M., 1997. Promotion by mixtures of dichloroacetic acid and trichloroacetic acid of N-methyl-N-nitrosourea-initiated cancer in the liver of female B6C3F1 mice. Cancer Lett. 115, 15–23. https://doi.org/10.1016/S0304-3835(97)04699-5.
Pérez-Albaladejo, E., Pinteño, R., Aznar-Luque, M.D.C., Casado, M., Postigo, C., Porte, C., 2023. Genotoxicity and endocrine disruption potential of haloacetic acids in human placental and lung cells. Sci. Total Environ. 879, 162981 https://doi.org/10.1016/j.scitotenv.2023.162981.
Pérez-Albaladejo, E., Casado, M., Postigo, C., Porte, C., 2024. Non-regulated haloaromatic water disinfection byproducts act as endocrine and lipid disrupters in human placental cells. Environ. Pollut. 342, 123092 https://doi.org/10.1016/j.envpol.2023.123092.
Plewa, M.J., Simmons, J.E., Richardson, S.D., Wagner, E.D., 2010. Mammalian cell cytotoxicity and genotoxicity of the haloacetic acids, a major class of drinking water disinfection by-products. Environ. Mol. Mutagen. 51, 871–878. https://doi.org/10.1002/em.20585.
Procházka, E., Escher, B.I., Plewa, M.J., Leusch, F.D.L., 2015. *In vitro* cytotoxicity and adaptive stress responses to selected Haloacetic acid and Halobenzoquinone water disinfection byproducts. Chem. Res. Toxicol. 28, 2059–2068. https://doi.org/10.1021/acs.chemrestox.5b00283.
Richardson, S.D., 2011. Disinfection By-Products: Formation and Occurrence in Drinking Water★★This article has been reviewed in accordance with the US EPA's peer and administrative review policies and approved for publication. Mention of trade names or commercial products does not constitute endorsement or recommendation for use by the US EPA. In: Encyclopedia of Environmental Health. Elsevier, pp. 110–136. https://doi.org/10.1016/B978-0-444-52272-6.00276-2.
Richardson, S.D., Plewa, M.J., 2020. To regulate or not to regulate? What to do with more toxic disinfection by-products? J. Environ. Chem. Eng. 8, 103939 https://doi.org/10.1016/j.jece.2020.103939.
Richardson, S.D., Fasano, F., Ellington, J.J., Crumley, F.G., Buettner, K.M., Evans, J.J., Blount, B.C., Silva, L.K., Waite, T.J., Luther, G.W., McKague, A.B., Miltner, R.J., Wagner, E.D., Plewa, M.J., 2008. Occurrence and mammalian cell toxicity of iodinated disinfection byproducts in drinking water. Environ. Sci. Technol. 42, 8330–8338. https://doi.org/10.1021/es801169k.
Richardson, S.D., DeMarini, D.M., Kogevinas, M., Fernandez, P., Marco, E., Lourencetti, C., Ballesté, C., Heederik, D., Meliefste, K., McKague, A.B., Marcos, R., Font-Ribera, L., Grimalt, J.O., Villanueva, C.M., 2010. What's in the Pool? A comprehensive identification of disinfection by-products and assessment of mutagenicity of chlorinated and brominated swimming Pool water. Environ. Health Perspect. 118, 1523–1530. https://doi.org/10.1289/ehp.1001965.
Rodríguez-Capote, K., Manzanares, D., Haines, T., Possmayer, F., 2006. Reactive oxygen species inactivation of surfactant involves structural and functional alterations to surfactant proteins SP-B and SP-C. Biophys. J. 90, 2808–2821. https://doi.org/10.1529/biophysj.105.073106.
Romero, F., Shah, D., Duong, M., Stafstrom, W., Hoek, J.B., Kallen, C.B., Lang, C.H., Summer, R., 2014. Chronic alcohol ingestion in rats alters lung metabolism, promotes lipid accumulation, and impairs alveolar macrophage functions. Am. J. Respir. Cell Mol. Biol. 51, 840–849. https://doi.org/10.1165/rcmb.2014-0127OC.
Rossner, P., Libalova, H., Vrbova, K., Cervena, T., Rossnerova, A., Elzeinova, F., Milcova, A., Novakova, Z., Topinka, J., 2020. Genotoxicant exposure, activation of the aryl hydrocarbon receptor, and lipid peroxidation in cultured human alveolar type II A549 cells. Mutation Research/Genetic Toxicology and Environmental Mutagenesis 853, 503173. https://doi.org/10.1016/j.mrgentox.2020.503173.
Sánchez-Soberón, F., Cuykx, M., Serra, N., Linares, V., Bellés, M., Covaci, A., Schuhmacher, M., 2018. In-vitro metabolomics to evaluate toxicity of particulate matter under environmentally realistic conditions. Chemosphere 209, 137–146. https://doi.org/10.1016/j.chemosphere.2018.06.065.
Schirmer, K., Chan, A.G.J., Greenberg, B.M., Dixon, D.G., Bols, N.C., 1997. Methodology for demonstrating and measuring the photocytotoxicity of fluoranthene to fish cells in culture. Toxicol. In Vitro 11, 107–119. https://doi.org/10.1016/S0887-2333(97)00002-7.
Schmidt, R., Meier, U., Markart, P., Grimminger, F., Velcovsky, H.G., Morr, H., Seeger, W., Günther, A., 2002. Altered fatty acid composition of lung surfactant phospholipids in interstitial lung disease. Am. J. Phys. Lung Cell. Mol. Phys. 283, L1079–L1085. https://doi.org/10.1152/ajplung.00484.2001.
Schnell, S., Olivares, A., Piña, B., Echavarri-Erasun, B., Lacorte, S., Porte, C., 2013. The combined use of the PLHC-1 cell line and the recombinant yeast assay to assess the environmental quality of estuarine and coastal sediments. Mar. Pollut. Bull. 77, 282–289. https://doi.org/10.1016/j.marpolbul.2013.09.047.
Tardiff, R.G., Carson, M.L., Ginevan, M.E., 2006. Updated weight of evidence for an association between adverse reproductive and developmental effects and exposure to disinfection by-products. Regul. Toxicol. Pharmacol. 45, 185–205. https://doi.org/10.1016/j.yrtph.2006.03.001.
Testerink, N., Van Der Sanden, M.H.M., Houweling, M., Helms, J.B., Vaandrager, A.B., 2009. Depletion of phosphatidylcholine affects endoplasmic reticulum morphology and protein traffic at the Golgi complex. J. Lipid Res. 50, 2182–2192. https://doi.org/10.1194/jlr.M800660-JLR200.
Thickett, K.M., McCoach, J.S., Gerber, J.M., Sadhra, S., Burge, P.S., 2002. Occupational asthma caused by chloramines in indoor swimming-pool air. Eur. Respir. J. 19, 827–832. https://doi.org/10.1183/09031936.02.00232802.
USEPA, 2010. US EPA, Comprehensive Disinfectants and Disinfection Byproducts Rules (Stage 1 and Stage 2): Quick Reference Guide. URL. https://bit.ly/2xXmFHP.
Villanueva, C.M., Font-Ribera, L., 2012. Health impact of disinfection by-products in swimming pools. Ann. Ist. Super. Sanita 48, 387–396. https://doi.org/10.4415/ANN_12_04_06.
Villanueva, C.M., Cordier, S., Font-Ribera, L., Salas, L.A., Levallois, P., 2015. Overview of disinfection by-products and associated health effects. Curr Envir Health Rpt 2, 107–115. https://doi.org/10.1007/s40572-014-0032-x.
Vlaanderen, J., Van Veldhoven, K., Font-Ribera, L., Villanueva, C.M., Chadeau-Hyam, M., Portengen, L., Grimalt, J.O., Zwiener, C., Heederik, D., Zhang, X., Vineis, P., Kogevinas, M., Vermeulen, R., 2017. Acute changes in serum immune markers due to swimming in a chlorinated pool. Environ. Int. 105, 1–11. https://doi.org/10.1016/j.envint.2017.04.009.
Wang, S., Zhang, H., Zheng, W., Wang, X., Andersen, M.E., Pi, J., He, G., Qu, W., 2013. Organic extract contaminants from drinking water activate Nrf2-mediated antioxidant response in a human cell line. Environ. Sci. Technol. 47, 4768–4777. https://doi.org/10.1021/es305133k.
Wang, W., Zhu, N., Yan, T., Shi, Y.-N., Chen, J., Zhang, C.-J., Xie, X.-J., Liao, D.-F., Qin, L., 2020. The crosstalk: exosomes and lipid metabolism. Cell Commun. Signal 18, 119. https://doi.org/10.1186/s12964-020-00581-2.
Werstuck, G.H., Lentz, S.R., Dayal, S., Hossain, G.S., Sood, S.K., Shi, Y.Y., Zhou, J., Maeda, N., Krisans, S.K., Malinow, M.R., Austin, R.C., 2001. Homocysteine-induced endoplasmic reticulum stress causes dysregulation of the cholesterol and triglyceride biosynthetic pathways. J. Clin. Invest. 107, 1263–1273. https://doi.org/10.1172/JCI11596.
Whitsett, J.A., Wert, S.E., Weaver, T.E., 2015. Diseases of pulmonary surfactant homeostasis. Annu. Rev. Pathol. Mech. Dis. 10, 371–393. https://doi.org/10.1146/annurev-pathol-012513-104644.
Wu, X., Chen, Z., Wu, Y., Chen, Y., Jia, J., Shen, N., Chiba, H., Hui, S.-P., 2022. Flazin as a lipid droplet regulator against lipid disorders. Nutrients 14, 1501. https://doi.org/10.3390/nu14071501.
Xiao, X., Yu, S., Li, S., Wu, J., Ma, R., Cao, H., Zhu, Y., Feng, J., 2014. Exosomes: decreased sensitivity of lung Cancer A549 cells to cisplatin. PloS One 9, e89534. https://doi.org/10.1371/journal.pone.0089534.
Yang, L., Chen, X., She, Q., Cao, G., Liu, Y., Chang, V.W.-C., Tang, C.Y., 2018. Regulation, formation, exposure, and treatment of disinfection by-products (DBPs) in swimming pool waters: a critical review. Environ. Int. 121, 1039–1057. https://doi.org/10.1016/j.envint.2018.10.024.
Yang, M., Zhang, X., Liang, Q., Yang, B., 2019. Application of (LC/)MS/MS precursor ion scan for evaluating the occurrence, formation and control of polar halogenated DBPs in disinfected waters: a review. Water Res. 158, 322–337. https://doi.org/10.1016/j.watres.2019.04.033.

Yeh, R.Y.L., Farré, M.J., Stalter, D., Tang, J.Y.M., Molendijk, J., Escher, B.I., 2014. Bioanalytical and chemical evaluation of disinfection by-products in swimming pool water. Water Res. 59, 172–184. https://doi.org/10.1016/j.watres.2014.04.002.

Yuan, J., Liu, H., Zhou, L.-H., Zou, Y.-L., Lu, W.-Q., 2006. Oxidative stress and DNA damage induced by a drinking-water chlorination disinfection byproduct 3-chloro-4-(dichloromethyl)-5-hydroxy-2(5H)-furanone (MX) in mice. Mutation Research/ Genetic Toxicology and Environmental Mutagenesis 609, 129–136. https://doi.org/10.1016/j.mrgentox.2006.05.011.

Zemski Berry, K.A., Murphy, R.C., Kosmider, B., Mason, R.J., 2017. Lipidomic characterization and localization of phospholipids in the human lung. J. Lipid Res. 58, 926–933. https://doi.org/10.1194/jlr.M074955.